ISSN : 0974 - 7486 Volume 12 Issue 3

Materials Science

An Indian Journal

Full Paper

MSAIJ, 12(3), 2015 [069-075]

Effect of heat treatment on the optical and morphological properties of iron oxide thin films prepared by spray pyrolysis

Salam Amir Yousif

Department of Physics, College of Education, University of Mustansiriyah, Baghdad, (IRAQ)

E-mail : Salamamir90@yahoo.com

ABSTRACT

Transparent thin films of Iron oxide have been deposited on a glass substrate at 400°C by simple and costeffective chemical spray pyrolysis technique. The effect of heat treatment on the optical and morphological properties of Fe_2O_3 thin films have been investigated. The transmittance of Fe_2O_3 thin films increase with increasing annealing temperature. The samples were also analyzed by atomic force microscopy (AFM) and they reveal grain morphology common for polycrystalline films. The root mean square roughness and grain size of the as grown and annealed Fe_2O_3 thin films have been studied.

INTRODUCTION

There are as many as 15 phases formed by Fe and O, as oxides of iron[1]. They are abundant in the earth's crust. They can be synthesized in pure, mixed oxides as well as doped structures. Iron oxide is used as an electrode in non-aqueous and alkaline batteries[2,3] and as a cathode in brine electrolysis[4]. Recently, Fe_2O_3 is found to have large third-order non-linear optical susceptibility and faster response time showing potential applications in optical computing [5]. It appears to have catalytic properties useful for N_2 fixation[6]. These oxides have been widely used in several industrial processes, such as dehydration, oxidation and Fischer–Tropsch synthesis[7–9]. Maghemite $\gamma - Fe_2O_3$ is ued in high-density magnetic recording devices[10]. Magnetite Fe_2O_4 in different forms is well understood for its giant magnetoresistance. Hematite is well known for its property of parasitic or canted magnetism. It is used in red pigments[11], anticorrosive agents[12], gas sensors to detect combustible gases, such as CH_4, C_3H_8, and i-C_4H_8[13,14] and electrochromic devices[15]. Due to the wide range of spectrum of applications, these oxides can be prepared in the form of powder, thin film and colloidal particles[16]. The most common oxides are hematite $(\propto -Fe_2O_3)$, maghemite $(\gamma - Fe_2O_3)$ and magnetite . These have different electrical, magnetic, electro-optical and chemical properties. Amongst these three common iron oxides hematite and maghemite have applications in gas sensors. The sensing mechanism in both cases is not the same. In $\gamma - Fe_2O_3$, it is from electron exchange between Fe^{3+} and Fe^{2+} and in $\propto -Fe_2O_3$ it is due to surface conductivity changes caused by the catalytic oxidation of reducing gases with chemisorbed oxygen-related species, such as O^- or O^{2-}[17]. Hematite $\propto -Fe_2O_3$ is n-type semiconductor with

hexagonal closed-packed crystal structure and has optical band gap around 2 eV, good chemical stability and appropriate valence band edges (i.e. +1.6 V/SCE at pH 14) for photo-induced oxygen evolution from water[18]. It has been tested as an electrode in photoelectrochemical (PEC) cell for energy conversion due to proper band gap[19]. Actual applications in devices require iron oxide in thin film forms. The thin film preparation can be broadly divided into physical and chemical methods. The physical methods result in excellent quality of thin films,but lack flexibility and cost effectiveness. The chemical methods like spin coating, dip coating, chemical solution deposition and spray pyrolysis are more flexible and economic. Preparations of spray pyrolytic thin films of $\propto -Fe_2O_3$ have been reported by various groups[20–24].

The present study deals with the spray pyrolytic deposition of iron oxide thin films from aqueous solution of iron chloride anhydrate. The effects of heat treatment on the optical and morphological properties of iron oxide thin films deposited by spray pyrolysis have been reported.

EXPERIMENTAL PART

Iron oxide (Fe_2O_3) thin films have been deposited on a glass substrate at a substrate temperature equal to 400^0C by a home-made chemical spray pyrolysis technique. The experimental setup and other details have been reported elsewhere[25]. A homogeneous solution with 0.1M was prepared by dissolving iron chloride anhydrate ($FeCl_3$) in distilled water at room temperature. The glass substrates were cleaned with ethanol and acetone for 15min by using ultrasonic cleaner and then rinsed in distilled water, and subsequently dried before deposition. The flow of the solution was 5–6ml/min and the oxygen was used as a carrier gas. The substrate to nozzle distance was fixed at 40cm, and the process involves spraying cycles of 8s, followed by periods with no spray of 90s. The surface morphology of Fe_2O_2 thin film was carried out by using atomic force microscopy (AFM, scanning probe microscope). The optical measurements of Fe_2O_2 thin film is calculated from the transmittance and absorbance spectrum at normal incidence in the range of (300 – 900 nm), by using UV-VIS spectrophotometer type (SHIMADZU) (UV-1600/1700 series).

RESULTS AND DISCUSSION

Optical properties

Transmittance (T)

The UV-visible transmittance spectra of Fe_2O_2 thin films as a function of wavelength for different annealing temperature have been shown in Figure 1. In all spectral regions except visible region, it is seen that the transmittance of the Fe_2O_2 films increases with increasing annealing temperature at,and in the visible region the transmittance of the films increases with increasing annealing temperature up to $500℃$ and then it decreases with increasing annealing temperature at ,and the average transmittance in the visible region (at 550 nm) has been found 50% for all samples. The transmittance value of 77% for the as-grown films is found to increase to 80% for the sample annealed at $600℃$ (at 900 nm). The decrease in the transmittance with increasing annealing temperature can be described to the decreasing Fe content as a result of the increasing of re-evaporation rate of Fe atoms from the iron oxide film[26].

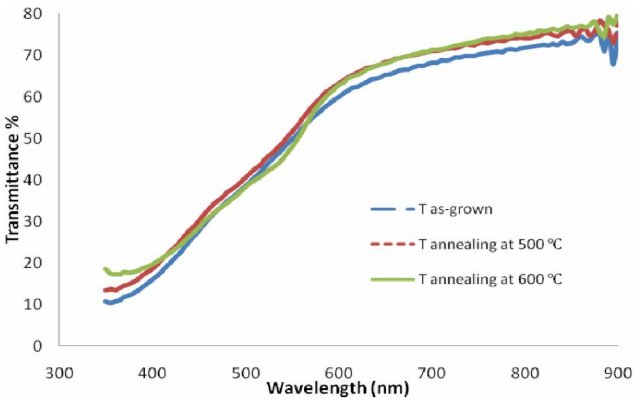

Figure 1: Transmittance spectra ofiron oxide thin films at different annealing temperature

Absorbance (A)

The absorbance spectra of Fe_2O_3 thin films as a function of wavelength deposited on a glass substrate at different annealing temperature are shown in Figure 2. In the high energy spectral range, where the film is strongly absorbed, and the absor-

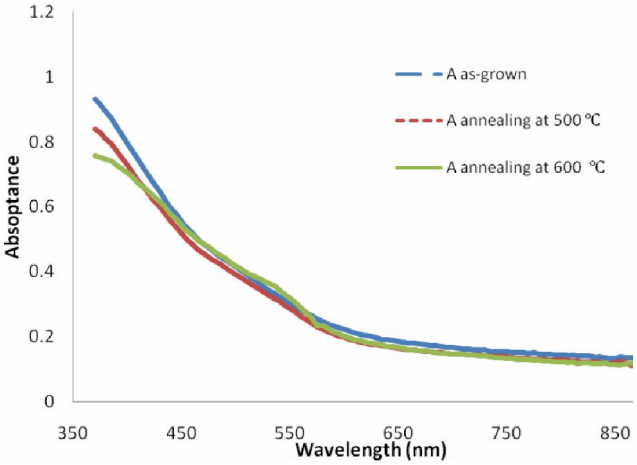

Figure 2 : Absorbance spectra ofiron oxide thin films at different annealing temperature

bance of films decreases with increasing annealing temperature.

Absorption coefficient (α)

The absorption coefficient (α) has been calculated from equation (1)[27,28].

$$\alpha = \frac{2.303\,A}{t} \qquad (1)$$

Where: A is the absorbance, t is the film thickness.

This coefficient depends on the incident photon energy (hυ), the energy gap of semiconductor and the type of the electronic transitions. Figure 3 shows the change of the absorption coefficient of the Fe_2O_3 thin films for different annealing temperature as a function of wavelength. It is observed that the absorption coefficient (α) decreases gradually with increasing annealing temperature, the value of absorption coefficient is greater than

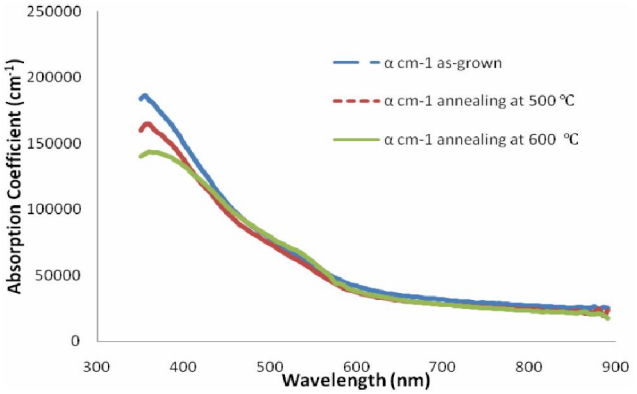

Figure 3 : Absorption coefficient ofiron oxide thin films at different annealing temperature

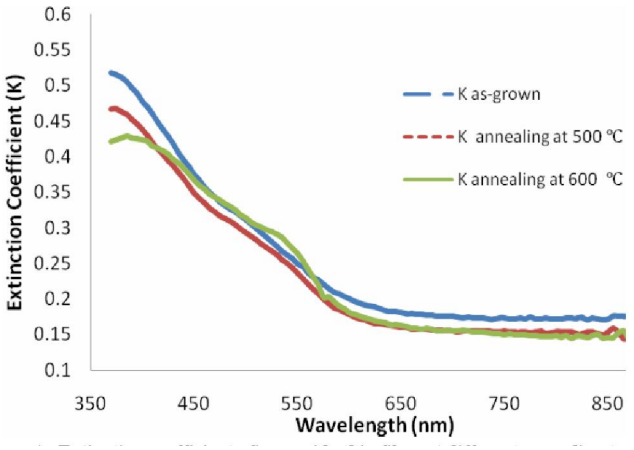

Figure 4 : Extinction coefficient ofiron oxide thin films at different annealing temperature

$(10)^4 cm^{-1}$) which indicates the strong possibility of direct electronic transitions.

Absorption Index (Extinction coefficient) (K)

The extinction coefficient (K) is calculated by equation (2)[27,28].

$$K = \frac{\alpha\lambda}{4\pi} \qquad (2)$$

Where: λ is the wavelength of incident photons.

Figure 4 shows the extinction coefficient versus wavelength plotted for different annealing temperature. This behavior agrees with the behavior of absorption coefficient which has a direct relation with (K) as in equation (2). The extinction coefficient decreases with increasing annealing temperature.

Optical conductivity ($\sigma_{optical}$)

The optical conductivity of thin films prepared at different annealing temperature has been calculated using equation (3)[29]:

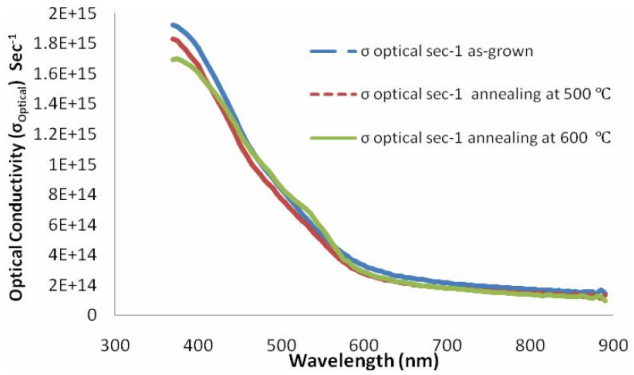

Figure 5 : Optical conductivity ofiron oxide thin films at different annealing temperature

$$\sigma_{optical} = \frac{\alpha n C}{4\pi} \quad (3)$$

Where: *n* is the refractive index, *C* is the speed of light.

Figure 5 shows the optical conductivity of thin films as a function of wavelength for different annealing temperature. It is observed that the optical conductivity decreases with increasing annealing temperature and the optical conductivity depends directly on the absorption coefficient as shown in equation (3). We can see that the optical conductivity increases with increasing the energy. This suggests that the increase in optical conductivity is due to electron excited by photon energy which leads to the increase in the concentration of charge carriers.

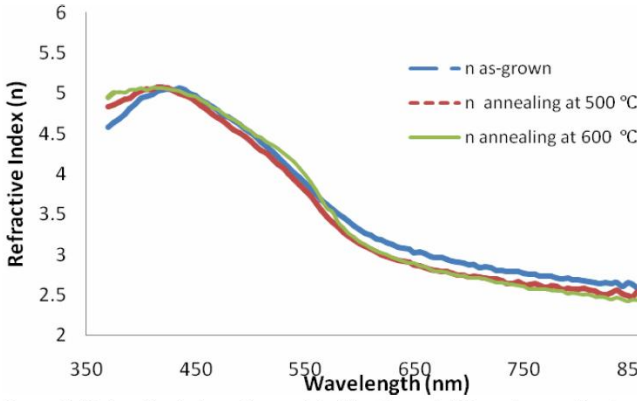

Figure 6 : Refractive index ofiron oxide thin films at different annealing temperature

Refractive index (n)

The refractive index (n) of Fe_2O_2 thin films is determined from equation (4)[30] as shown in Figure 6.

$$n = \left[\left(\frac{4R}{(R-1)^2}\right) - K^2\right]^{1/2} - \frac{R+1}{R-1} \quad (4)$$

Where: *R* is the reflectance

All films show similar behavior in refractive index. The refractive index of Fe_2O_2 thin films decreases with increasing annealing temperature. It is concluded that the reflection index highly depend on the production technique, surface roughness, grain boundaries and morphologies of the produced films, and these properties change with annealing temperature.

Real and imaginary part of dielectric constant (ε_1),(ε_2)

An absorbing medium is characterized by a complex dielectric constant. The real and imaginary parts of dielectric constant of Fe_2O_2 thin film has been calculated using equations (5), (6)[31].

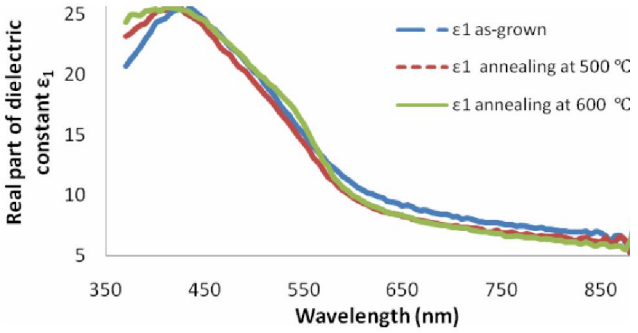

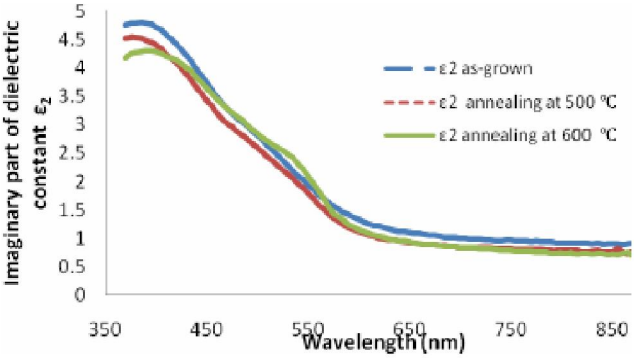

Figure 8 : Imaginary part of dielectric constant ofiron oxide thin films at different annealing temperature

$$\varepsilon_1 = n^2 - K^2 \quad (5)$$

$$\varepsilon_2 = 2nK \quad (6)$$

The real and imaginary parts of dielectric constant as a function of wavelength of Fe_2O_2 thin films at different annealing temperature are shown in Figs. 7, 8 respectively. It is found that the real and imaginary parts of the dielectric constant of Fe_2O_2 thin films decrease with increasing annealing temperature.

Figure 9shows the plot of $(\alpha h\vartheta)^2$ against $h\vartheta$ for the as-grown and annealed films. The optical absorption coefficient values are of the order of $10^4 cm^{-1}$ for all the films. The nature of the transitions and the band gap is calculated by using the following equation,

$$\propto = constant \frac{(h\vartheta - E_g)^X}{h\vartheta} \quad (7)$$

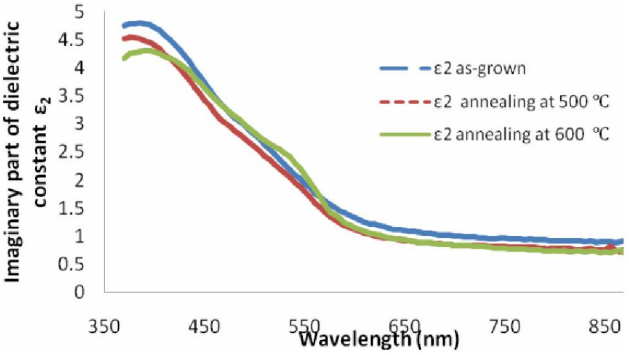

Figure 9 : Optical band gap ofiron oxide thin films at different annealing temperature

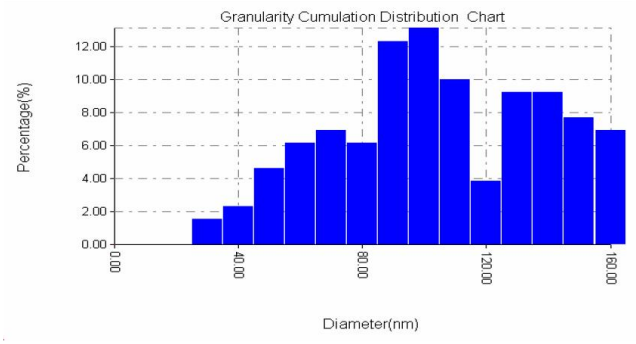

Figure 11 : Granularity distribution of as-grown Fe_2O_3 thin film deposited at

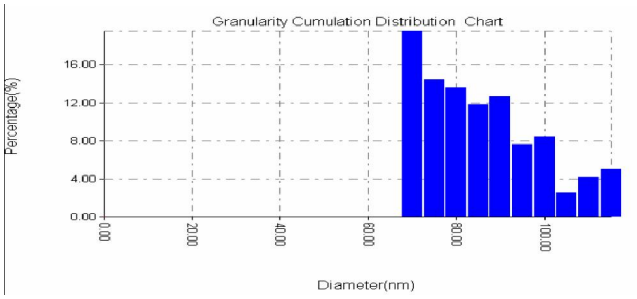

Figure 13 : Granularity distribution ofFe_2O_3 thin film annealed at 500℃

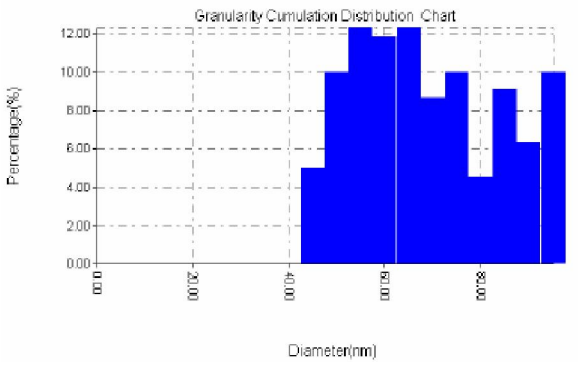

Figure 15 : Granularity distribution ofFe_2O_3 thin film annealed at 600℃

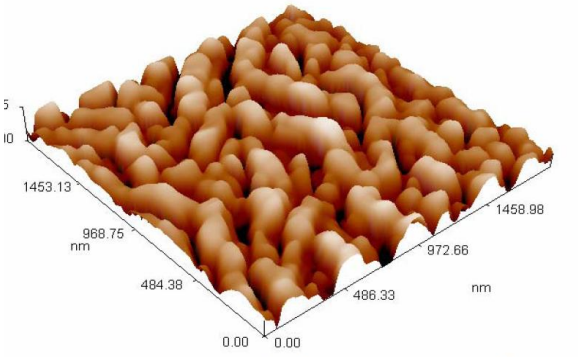

Figure 10 : AFM images of as-grownFe_2O_3 thin film deposited at 400℃

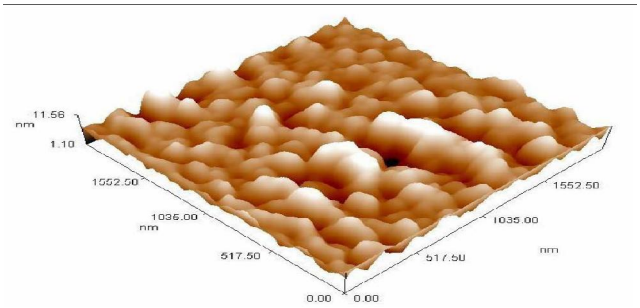

Figure 12 : AFM images of Fe_2O_3 thin film annealed at 500℃

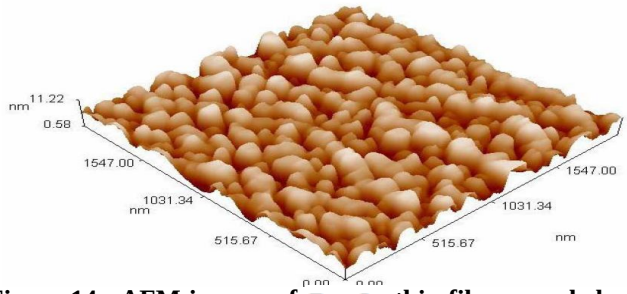

Figure 14 : AFM images of Fe_2O_3 thin film annealed at 600℃

Where:*x = 1/2* for direct transitions and *x= 2* for indirect transitions.

The plot of $(\alpha h\vartheta)^2$ against hγ (Figure 5) islinear in nature, indicating that the material ofthe films has a direct optical band gap. The extrapolation of the straight line to $\alpha = 0$ gives a direct band gap equal to 2.68eV for the as-grown thin film, and this value decrease with increasing annealing temperatureand takes the values 2.64, 2.46eV at annealing temperature $500°C, 600℃$ respectively,which is consistent with the another report[32].

Morphology

Figures. 10, 12, 14 show the AFM images ofas-grown and annealed Fe_2O_2 thin films. As shown in the figures, the surface morphology changed with the varying annealing temperatures. The films reveal homogenous surface and the grains were elongated from the inner towards the surface andthe root mean square (RMS) roughness of theas-grown film was 1.33nm. This is attributed to the fact that the surface diffusion was sufficient due to the deposition temperature. However, after annealing the film at 500, 600°C under ambient atmosphere, the rough ofthe surface increases with increasing annealing temperature. The root mean square and grain size of the as grown and annealed Fe_2O_2 thin films have been listed in TABLE 1. The grain size of Fe_2O_2 thin films were evaluated at 99, 83, 66 nm for as-grown and annealed films as shown in TABLE 1. Grain size was less than 100 nm which confirms the presence of nanostructures. AFM study reveals that the roughness of the film is dependent on the annealing temperature.

TABLE 1: RMS roughness, Grain size and peak-peak height of iron oxide film

Annealing temperature ℃	RMS roughness (nm)	Grain size (nm)	Peak-Peak eight (nm)
as-grown 400	1.33	99	5.95
500	1.77	83	11.56
600	2.02	66	11.25

CONCLUSION

Fe_2O_3 thin films have been deposited successfully on a glass substrate by spray pyrolysis technique. The transmittance of the Fe_2O_3 films increases with increasing annealing temperature, and in the visible region the transmittance of the films increases with increasing annealing temperature up to $500℃$ and then it decreases with increasing annealing temperature at $600℃$. The decrease in the transmittance with increasing annealing temperature can be described to the decreasing Fe content as a result of the increasing of re-evaporation rate of Fe atoms from the iron oxide film. The direct band gap equal to 2.68eV for the as-grown thin film, and this value decrease with increasing annealing temperature and takes the values 2.64, 2.46eV at annealing temperature respectively. The films reveal homogenous surface and the grains were elongated from the inner towards the surface andthe root mean square (RMS) roughness of theas-grown film was 1.33nm. This is attributed to the fact that the surface diffusion was sufficient due to the deposition temperature. However, after annealing the film at 500, 600°C under ambient atmosphere, the rough of the surface increases with increasing annealing temperature.

REFERENCES

[1] R.M.Cornell, U.Schwertmann; The Iron Oxides, second Edition, Wiley-VCH, 11 **(2003)**.
[2] S.Kenichi, J.Akinide, T.Kiyohide, Japan Patents, **61(24)**, 147 **(1986)**.
[3] F.Sanehiro, Y.Sejji, N.Toshiyuki; Japan Patents, **62(160)**, 651 **(1981)**.
[4] K.Keiji, M.Itsuaki; Japan Patents, **79(106)**, 78 **(1979)**.
[5] M.Ando, K.Kandono, M.Haruta, T.Sakaguchi, M.Miya; Nature, **374**, 625 **(2002)**.
[6] M.M.Khader, N.N.Lichtin, G.H.Vurnes, M.Salmenon, G.A.Somoraj; Langmuir, **3**, 303 **(1987)**.
[7] L.Daza, C.M.Rangel, J.Baranda, M.T.Casais, M.J.Martinez, J.A.Alonso; J.Power Sources, **86**, 329 **(2000)**.
[8] H.H.Kung; Transition Metal Oxides: Surface Chemistry and Catalysis, Elsevier, Amsterdam, **(1989)**.
[9] C.K.Rofer-Depoorter; Chem.Rev., **81**, 447 **(1981)**.
[10] H.Hibst, E.Schwab; In: R.W.Cahn, P.Hassen, E.J.Kramer, (Eds); Magnetic Recording Materials in Materials Science and Technology, VCH Weinheim, **3B**, 212 **(1994)**.
[11] M.Jansen, H.P.Letschert; Nature, **404**, 980 **(2000)**.
[12] J.M.West; Basic Corrosion and Oxidation, second Edition, Ellis Horwood Ltd., Chchester, **(1986)**.
[13] M.Matsuoka, Y.Nakatani, H.Ohido; Nat.Tech.Rep., **24**, 461 **(1978)**.
[14] L.Huo,W.Li, L.Lu, H.Cui, S.Xi, J.Wang, B.Zaho, Y.Shen, Z.Lu; Chem.Mater., **12**, 90 **(2000)**.
[15] B.Orel, M.Macek, F.Svegl; Thin Solid Films, **246**,

131 **(1994)**.
[16] B.Pal, M.Sharon; J.Chem.Technol.Biotechnol., **73**, 269 **(1998)**.
[17] Z.Tianshu, P.Hing, Z.Ruifang; J.Mater.Sci., **35**, 1419 **(2000)**.
[18] J.H.Kennedy, D.J.Dunnwald; J.Electrochem.Soc., **130**, 1013 **(1983)**.
[19] U.Bjorksten; J.Moser, M.Gratzel; Chem.Mater., **6**, 858 **(1994)**.
[20] K.Nomura, Y.Ujihira, K.Itoh, K.Honda; Thin Solid Films, **128**, 225 **(1985)**.
[21] Y.T.Qian, C.M.Niu, C.Hanngan, S.Yang, K.Dwight, A.Dwight; J.Solid State Chem., **92**, 208 **(1991)**.
[22] T.Young Ma, I.C.Lee; Mater.Sci.: Mater.Electr., **15**, 775 **(2004)**.
[23] A.A.Akl; Appl.Surf.Sci., **221**, 319 **(2004)**.
[24] S.U.M.Khan, J.Akikusa; J.Phys.Chem., **B103**, 7184 **(1999)**.
[25] P.S.Patil; Mater.Chem.Phys., **59**, 185 **(1999)**.
[26] D.Hwang, M.Jeong, J.Myoung; Appl.Surf.Sci., **225**, 217 **(2004)**.
[27] B.L.Sharma, R.K.Purohit; Semiconductor Hetrojunction, Pergomon Press, New York, **(1974)**.
[28] L.K.Chopra; Thin film phenomena, Mc Graw Hill Book Company, **(1969)**.
[29] Abakaliki, Nigeria; The Pacific Journal of Science and Technology, **7**, 1 **(2006)**.
[30] J.Parkes, R.D.Tomlinson, M.J.Hamphire; J.Solid State Electronic, **16**, 773 **(1973)**.
[31] M.Balkanski, R.F.Wollis; Semiconductor physics and application, Oxford University press, **(2000)**.
[32] R.A.Ismail, Y.Najim, M.Ouda; e-J.Surf.Sci.Nanotech., **6**, 96 **(2008)**.